Field testing autogenic storage thresholds for environmental signals in the strata of the Mississippi River Delta, U.S.A.

Udita Mukherjee† and Kyle M. Straub

Department of Earth and Environmental Sciences, Tulane University, New Orleans, LA 70118, U.S.A.

†Present Address: Department of Geoscience, University of Wisconsin, Madison, WI 53706, U.S.A.

Correspondence to: Udita Mukherjee (umukherjee@tulane.edu)

ABSTRACT

Sediments transported from source terrains to depositional sinks carry environmental signals, which may or may not be preserved in stratigraphy. Recently developed theory suggests storage thresholds for environmental signals are set by the internal dynamics of sediment transport systems. For the first time, we explore this theory by testing whether changes in relative sea level (RSL) of various scales produce detectable signals stored in field scale stratigraphy. This field test builds on results from physical experiments where identifiable stratigraphic signals of RSL change were only produced from RSL cycles with magnitudes and/or periodicities greater than the spatial and temporal scales of the internal dynamics of deltas. Published long term sedimentation rates and sea level reconstructions suggest that the Mississippi River Delta (MRD) should be a good place to study sea level signal storage thresholds. We use publicly available seismic volumes from NAMSS-USGS to study how and if signals of paleo-sea level change are stored in strata of the MRD, comparing strata of the late Miocene (LM) and early Quaternary (EQ). Comparison of the amplitude and period of cycles in these two time periods, constrained by micropaleontological data, predicts storage of RSL signals in EQ strata, but not in the LM strata. This is confirmed as we show that signals of larger amplitude EQ RSL cycles are preserved in the MRD, but smaller amplitude LM signals are not detectable. This study adds field scale observations that quantify the intermingling of stratigraphic products of internal dynamics with products of RSL change over geological timescales.

INTRODUCTION

Relative sea level (RSL) change can be connected to climate change and is used as a proxy to reconstruct past change in global temperature, melting of ice sheets, tectonics and paleogeography (Haq *et al.*, 1987; Fairbanks, 1989; Haq, 1991; Clark *et al.*, 2004; Alley *et al.*, 2005). Signals of sea level change through Earth history are stored in strata and decoding these signals can help us interpret paleoclimate. Changes in RSL also drive changes in the dynamics of Earth's surface (e.g., channel migration rate) which gets recorded in strata. RSL change is one of the most important external (allogenic) forcings affecting sediment deposition rates and stratigraphic architecture of continental margin systems. Paleo-RSL change has commonly been studied with sequence stratigraphy, a branch of stratigraphy that connects depositional patterns and erosional surfaces preserved in marginal marine strata to allogenic forcings like RSL change (Posamentier & Vail, 1988; Van Wagoner *et al.*, 1988; Catuneanu *et al.*, 2009). Many paleo-environmental interpretations that utilize sequence stratigraphic methods emphasize landscape responses to RSL change to explain stratigraphic architecture (Van Wagoner, 1995; Catuneanu *et al.*, 2009; Bhattacharya, 2011; Blum *et al.*, 2013). Falling RSL is connected to incision, formation of valleys, and a basinward shift of depositional facies. In contrast, rising RSL is thought to shift deposition landward, with eventual valley filling and preservation of paleovalleys in strata (Posamentier & Vail, 1988).

Signals of changing sea level are thought to be abundant in marginal marine strata (Jelgersma, 1961; Blum & Törnqvist, 2000; Miller *et al.*, 2005; Khan *et al.*, 2019). However, recent work questions the ability of some basins to record detectable signals of certain RSL events. For example, Li et al. (2016) and Yu et al. (2017), using physical experiments, explored the distortion and reduction in detectability of RSL signals by processes that are intrinsic to sediment transport systems (autogenic processes). This contrasts with many interpretations of sequence-stratigraphic patterns that emphasize deterministic system responses to past RSL change and the resultant stratal architecture (Posamentier & Vail, 1988; Posamentier & Allen, 1992; Catuneanu *et al.*, 2009). The distinction between allogenic and autogenic controls on sediment transport and the comparison of scales of the resulting stratigraphic features are important questions worth exploring (Best & Ashworth, 1997; Ganti *et al.*, 2019). Some observational work (Trower *et al.*, 2018) has even applied aspects of stochastic signal degradation theory (signal shredding theory) at field scale.

Signal shredding describes how signals can be destroyed due to sediment storage and release and the study of this is still a comparatively new area of research (Jerolmack & Paola, 2010; Romans *et al.*, 2016). Signal shredding can result from the degradation of signals during transport or burial and from the intermingling of the products of allogenic and autogenic surface processes in strata. Signals of environmental change can be spread temporally as well as spatially in a source to sink system due to autogenics. This is referred to as ‘smearing of signals’ over landscapes as well as the strata (Jerolmack and Paola, 2010). This smearing results from the temporary storage in landforms like bed and bar forms, and due to flux of sediment out of channels to depositional environments like floodplains. This temporary storage also results in a smearing of signals in time as sediment liberation during episodes of erosion results in a distribution of transit times for sediment routed from a source to a sink (Castelltort & Van den Driessche, 2003; Romans *et al.*, 2016; Burgess *et al.*, 2019; Lazarus *et al.*, 2019). Significant smearing of signals across time and space can make it impossible to piece together the depositional clues one uses to infer paleo-environmental change.

However, not all environmental signals travel along the full length of the transport system before deposition. A good example of this is a change in relative sea level, as it is felt by the transport systems first at the shoreline, from where a signal can be generated that propagates both up and down the system (Fisk, 1954; Lamb *et al.*, 2012; Voller *et al.*, 2012). While signals can propagate over the Earth’s surface along a dominant sediment transport path, they can also travel vertically into strata. In the case of sea level change, this vertical signal propagation into the stratigraphic record can occur with no or limited horizontal propagation (Vail, 1987; Posamentier & Vail, 1988; Van Wagoner *et al.*, 1988). During the burial process, signals first reside in the active layer (layer still susceptible to reworking via autogenic processes) where they can be degraded by the burial and/or incision process. If this degradation is significant, the resultant stratigraphy may not preserve detectable evidence of changing RSL. Only when these deposits are buried to a depth sufficient to be shielded from autogenic surface processes are they safe from further autogenic degradation (Mohrig *et al.*, 2000; Olariu & Bhattacharya, 2006; Straub *et* *al.*, 2009). We follow the language of Straub et al. (2020) and differentiate a “transport shredder” from a “stratigraphic shredder”. The stratigraphic shredder is associated with the vertical burial processes of environmental signals. This work will focus on degradation of RSL signals resulting from the burial processes, specifically for signals with short horizontal transit distances (RSL signals preserved near paleo-shorelines).

Studying stratigraphic signal storage with seismic data from the Mississippi delta

When it comes to exploration of signal shredding theory at field scales, little has been done because of scarce publicly available 3D data that is of decent areal coverage and also is sufficiently dated. Li et al. (2016) and Yu et al. (2017) calculated the preservation potential of RSL signals for a database of field scale deltaic systems. This analysis suggested that the present-day Mississippi River Delta (MRD) is a good place to test signal-shredding theory. RSL cycles from two time periods in the large basin of the MRD are hypothesized to reside on either side of the stratigraphic signal detection divide. Specifically, we compare strata deposited during the early Quaternary (EQ), when RSL cycled with large amplitudes, and the late Miocene (LM) that had much lower amplitude RSL cycles (Lisiecki and Raymo, 2005; Miller et al., 2005). The past physical and numerical experiments used to test the theory assumed that the major trunk system in a sedimentary basin sets the fidelity of the entire basin. These experiments were fed by a single delivery point for water and sediment to the experimental basins (Li *et al.*, 2016; Yu *et al.*, 2017). However, we recognize that the larger MRD basin contains both a trunk channel system and smaller coastal river basins. Thus, we also explore the ability to detect signals in deposits of these small coastal systems that exist in the larger basin. We hypothesize that EQ RSL signals will be preserved in strata deposited from both the small and large systems. In contrast, signals of LM RSL change are expected to be preserved in strata deposited from the smaller coastal systems, but not in the strata tied to the trunk system.

We use publicly available seismic volumes from the National Archive of Marine Seismic Surveys, under USGS (NAMSS-USGS) to measure the dimensions of stratigraphic features resulting from channelized flow in the stratigraphy of the EQ and the LM. We aim to ascertain if any of these channelized geobodies (CBs) can be categorized as paleovalleys in the sedimentary packages from the two time periods of interest, which is indicative of the storage of sea level signals. For this, we define autogenic scales first, in the form of dimensions of the present-day Mississippi river and look for variations away from autogenic scales. To our knowledge this is the first field scale study to test signal shredding theory.

THEORETICAL BACKGROUND

Following theory developed by Li et al. (2016) and Yu et al. (2017), amplitude and time-periods of RSL cycles are compared with autogenic time and space scales for deltaic stratigraphy. *H**, a dimensionless length scale and *T**, a dimensionless timescale (Li et al., 2016; Yu et al., 2017) are defined as:

$$H^* = \frac{R_{RSL}}{H_C} \quad \text{(EQ. 1)}$$

$$T^* = \frac{T_{RSL}}{T_C} \quad \text{(EQ. 2)}$$

where R_{RSL} is the range of an RSL cycle (i.e. difference in elevation of sea-level between highstand and lowstand), H_C is the depth of the largest autogenic channels, which can be as large as $3H_{mean}$ (Ganti et al., 2014), T_{RSL} is the period of an RSL cycle and T_C is the compensation timescale, which is the time for deposits of autogenic surface processes to average out such that an isopach reflects an accommodation generation pattern (Wang et al., 2011). The compensational timescale can be estimated as:

$$T_C = \frac{l}{\bar{r}} \quad \text{(EQ. 3)}$$

Where $\bar{r}$ is the long-term sedimentation rate, and *l* is the maximum autogenic vertical roughness scale in a region of study. *l* has been approximated by H_C in several experimental studies. However, this scale for some settings might be larger than H_c, due to the presence of features like delta foresets that could introduce even larger roughness scales into a system (Trampush et al., 2017).

Results from physical experiments suggest that deltas experiencing RSL cycles characterized by *H** and/or *T** >>1 preserve sea level signals in their strata. However, in systems where both *H** and *T** <<1 signals of RSL cycles are either absent or of similar scale to products of autogenic processes, making them difficult to detect.

Predicting signal detectability requires estimates of autogenic system scales. Prior studies suggested that the present-day Mississippi River is largely the result of autogenic processes in the Holocene (Blum & Törnqvist, 2000; Li *et al.*, 2016; Yu *et al.*, 2017). Such morphometric scales from the modern system are used to estimate autogenic scales. We use maps of the lower Mississippi River (Nittrouer, 2013; Fernandes *et al.*, 2016) to estimate an H_c of ~70m. Prior estimates of a long term sedimentation (or subsidence) rate of 0.23 m/kyr for this system came from biostratigraphic dates in the strata below the current Bird's foot of the MRD (Straub et al. 2009). Using these values, estimates of *H** and *T** for the MRD EQ are 1 and 0.1, respectively, whereas for LM strata, *H** and *T** are estimated at 0.2 and 0.1, respectively.

<u>Expected RSL signals in the strata</u>

The H^*-T^* framework gives us a tool to quantitatively compare the scales of allogenic environmental forcings with the scales of local autogenic signals. The H^*-T^* regime can aid prediction of not only the presence, but an expected type of RSL signal in strata, depending on the RSL signals falling in the different quadrants of the H^*-T^* space. H^* and T^* are inversely proportional to autogenic channel depths. A channel that plots in the quadrant defined by both H^* and $T^*>1$ should produce CBs that are both deeper and wider than their autogenic representations. Incision and formation of paleovalleys should also drive basinward movement of the depocenter. In the case of $H^*>1$ and $T^*<1$, we suggest the dominant signal will be an increase in CB thickness relative to autogenic products as the high RSL cycle amplitude will be linked to incision, but there will be limited time to widen the valley out during a cycle. For $T^*>1$ and $H^*<1$, one can expect to see wider CBs and more distal sediment deposition, but not necessarily channel bodies that are thicker than autogenic scales. In the case of H^* and T^* both being less than 1, the RSL signal will be susceptible to shredding.

STUDY AREA

The northern Gulf of Mexico is a stable divergent continental margin (Galloway, 1989) and has been the major sink for sediments sourced from the continental United States for the past 65 million years (Galloway et al., 2011) (Fig. 1a). While the sediment routing and drainage patterns of the Mississippi River changed through time, the MRD has been active for most of the last 65 Myrs, except for the Eocene epoch (Blum and Pecha, 2014; Blum et al., 2017; Galloway et al., 2011; Xu et al., 2017). During the LM and EQ time-periods, the terminus of the Mississippi River was one of the principal depocenters in the Gulf of Mexico (Bentley Sr et al., 2016; Blum et al., 2017; Galloway et al., 2011; Wu, 2004; Xu et al., 2017).

The present axis of the MRD has been in place since the Miocene. During this time, RSL cycles ranged from ~10-20 m with a cycle period of ~40 kyr (Lisiecki and Raymo, 2005; Miller et al., 2005; Raymo et al., 2006). The shelf-edge prograded by ~200 km and the nucleus for the present alluvial system, with the deepwater system in the Gulf of Mexico, was set up (Galloway et al., 2011; Winker, 1982). This coastal and deepwater sediment accumulation led to the formation of a composite delta system (Bentley Sr et al., 2016; Combellas-Bigott and Galloway, 2006; Galloway et al., 2000; Galloway et al., 2011; Winker, 1982; Wu, 2004).

Throughout much of the early Quaternary (2.5-0.77 Ma), RSL cycles were dominated by a 40 kyr period. This transitioned to a dominant period of 100 kyrs in the Pleistocene (Imbrie and Imbrie, 1980; Lisiecki and Raymo, 2005; Miller et al., 2005; Raymo et al., 2006). In the Gulf of Mexico, this transition is temporally linked to the presence of the foraminifera *Trimosina* A, typically dated at ~0.6 Ma (Galloway et al., 2000). EQ RSL cycles had a range of ~60-70 m (Lisiecki and Raymo, 2005; Miller et al., 2005; Raymo et al., 2006). During this period, the mean Quaternary shoreline rested around the present-day mid-shelf with superimposed fluctuations due to the RSL forcing (Blum et al., 2009).

The MRD basin has been impacted by shifts in climate and associated sea level change over a range of timescales (Buzas-Stephens et al., 2014). Changes in sediment flux from the hinterland due to changes in climate, tectonics, and geology in the drainage basins of the rivers have influenced sedimentation patterns (Anderson et al., 2016). The MRD is also highly influenced by variable basin subsidence in space and time, driven by sediment compaction and glacial and sedimentary isostatic adjustment. Over long timescales, depositional patterns in the GoM are influenced by structural processes, including deep-seated subsidence caused by cooling of the crystalline basement and movement of gravity tectonic structures (e.g., Jurassic Louann salt). The salt and the structures created by its movement add to the overall complexity of the GoM, in terms of creation of accommodation and rapid subsidence in the shelf. This affects the thickness of strata from the Mesozoic through the Quaternary (Combellas-Bigott and Galloway, 2006; Diegel et al., 1995; Galloway et al., 2000; Peel et al., 1995; Peel, 2014; Winker, 1982). Care has been taken to exclude manifestations of the salt structures and faults during seismic interpretation (Fig. 2). Other factors influencing marginal marine sedimentation patterns and physiography in this area include differential fluvial fluxes (Olariu and Steel, 2009) and oceanographic currents and circulation systems (Anderson et al., 2004; Anderson et al., 2016). However, possibly the largest environmental forcing at this site is eustatic sea-level (Fisk, 1954; Blum & Törnqvist, 2000), given its influence on the location of shorelines and the change of transport physics that occur across this boundary .

Data and Methods

Micropaleontological data

To meaningfully analyze the geological history imaged with the seismic data from the study area, different stratigraphic packages need assigned ages. There is limited data on the age of strata in the study area over the age range we query. However, for this study, the precise age of strata that might allow one to identify the signal of a specific sea level cycle is not necessary. Rather, sufficient dating that allows for the general age of strata (+/- 1 Myrs) is necessary. This allows us to identify the general scale (amplitude and period) of sea-level fluctuations that were ongoing at the time of deposition. By using planktonic foraminifera available from a well in the study area, an age-depth model is generated (Fig. 1b). Specifically, using the depth and age ranges of the microfossils *Lenticulina* and *Bigenerina floridana* in conjunction with the modern

Earth surface, the estimated sedimentation rate for the study area is 0.54 m/ka. Using this rate, the estimated local H^* and T^* values for the EQ are 1 and 0.8, respectively, whereas for LM stratigraphy H^* and T^* are 0.1 and 0.3, respectively.

<u>*Present-day Mississippi channel width*</u>

The dimensions from the present-day Mississippi channel were compared to the EQ and LM CB dimensions. Data defining the depth and width of the present-day Mississippi channel, as measured from Head of Passes, are reported in Nittrouer et al. (2012) (collected by U.S. Army Corps of engineers (USACE; data collected 1974–1975; found in Harmar, 2004, appendix)). This survey data included channel cross-sections on average every 312 m, which covers the transition from the normal-flow stretch through the backwater reach. The difference in channel levee crest and thalweg elevations for every transect is reported as the modern channel depth. The width data comes from these same profiles and is measured from one levee crest to the levee crest on the opposite channel margin along a perpendicular transect. All the elevation data are expressed in meters above mean sea level and were converted from the data referenced to NGD 1929. Distributions of channel depths and widths are then generated for the full lower 800 river kms and for just the lower 200 river kms.

The distance of the farthest landward edge of the seismic volume from the average LM and average EQ shoreline are ~120 kms and ~50 kms, respectively. These are calculated based on the perpendicular distance of the center of the seismic volume from the closest EQ and LM shoreline positions (Galloway et al., 2000). Acknowledging that sea level cycles, sediment supply and accommodation can alter these distances significantly, this is an estimate of the average distance separating the study region from the shoreline over the time periods explored, and comparable to the 200 river kms of the present-day Mississippi channel belt.

Channel belt width data from Fernandes et al. (2016) is then used to compare EQ and LM CB dimensions with modern autogenic values. Again, distributions of CB scales are made both for the lower 800 kms and lower 200 kms. Given the time integrative nature of strata, the scales of interpreted CBs are likely more analogous in their formative processes to modern channel belts, compared to the geometry of the river itself.

<u>*Seismic dataset*</u>

The publicly-available 3D seismic cube (~980 sq km) used here to calculate distributions to describe widths and depths of CBs, covers a swath of the current continental shelf, just west of the Mississippi Canyon (Figs. 1&2). This region is near the center of the long-term MRD basin (Fig 1a) and as such received sediments through the LM and EQ time-periods (Galloway, 2008; Galloway et al., 2000; Galloway et al., 2011). The seismic volume was collected in 1993 for oil and gas exploration purposes. The inline and crossline spacings are 25 m and the sample interval is 4 milliseconds. The frequency content of the seismic volume averages ~35 Hz with a falloff on the high frequency end at ~65 Hz, with a theoretical vertical resolution of 7-14 m. Using the sedimentation rate calculated, EQ strata is in a depth range of 0.5-1 km, corresponding to an age range of approximately 1-0.8 Ma. For LM strata, the depth range is 3.5-4 km, corresponding to an age range of approximately 6-6.3 Ma. However, the uncertainties on these numbers can be expected to be large, based on change in sedimentation rates in the system.

Seismic waves reflect and refract along geophysical boundaries, many of which are associated with lithologic boundaries in the subsurface. Using this principle, the seismic cube was utilized to interpret CBs of different dimensions from the EQ and LM. For this study, we define channelized bodies as any geobody constructed from channelized processes. This term encompasses channels, channel belts, and paleo-valleys. We emphasize and acknowledge that this is a slightly different use of this term than commonly used in the literature. These CBs were interpreted from both horizontal and vertical seismic sections. Interpretation and mapping of the smaller channel features is easier in approximately horizontal time slices compared to vertical sections due to data resolution and typical aspect ratio of CBs (width ≫ depth). CB margins are interpreted on horizontal (time) sections using a variance attribute that accentuates edges or discontinuities in the seismic data (Figs. 3&4). Windows of ~100 milliseconds, which corresponds to about 300 thousand years of age and close to 100m of thickness, are identified for both the EQ and LM time-periods. This thickness is roughly equivalent to the compensation scale of the basin (i.e., approximately equal to the maximum depth of the modern Mississippi River). Each of these windows is then divided into ~12 time-slices with a spacing of ~8 milliseconds, with the LM sections flattened on a regional surface. For every time slice, discontinuities interpreted as CB margins, were mapped. CB margins are described as two linear features that run approximately parallel to each other with a sinuosity to channel width relationship similar to modern-day channels and channel belts (Leopold and Wolman, 1960). Some CBs were also mapped in cross-section where they were identified with paired inclined reflectors that truncate underlying seismic horizons. This mapping process produced a database that consists of 821 CBs: 431 (50 vertically resolvable from seismic data) from EQ and 390 (33 vertically resolvable from seismic data) from LM.

Calculation of CB dimensions

The dimensions of CBs can hold valuable clues about their origins, including the influence of sea level cycles, and clues for the presence of allogenic vs allogenic signals. Using the interpreted CB margins, channelized-body widths were calculated using a Python based script designed by Sylvester and reported on in Sylvester et al. (2021). The detailed script and explanation for the width calculation is available at https://github.com/zsylvester/channelmapper.

Following the Gibling (2006) framework, geobodies produced by channelized transport processes in coastal settings can be placed into four bins: alluvial valley fills, delta distributaries, meandering channels and braided channels. The calculated CB widths were compared with the typical widths of these types of features (Table 1) and then interpreted accordingly.

We also estimate thicknesses of CBs, specifically maximum thicknesses, which is necessary to calculate H^* and T^*. CBs with thicknesses below the vertical resolution of the seismic volume cannot be directly interpreted. For each CB that could not be imaged in the vertical, we used the database from Gibling (2006) to calculate a theoretical maximum CB thickness. Depending on the type of CB, the width was combined with the associated width:thickness ratios to arrive at a theoretical maximum thickness (Table 1). For vertically resolvable CBs, the difference between the maps of the CB base and an approximate top envelope gives an approximate maximum thickness. The top envelope is constructed by connecting the top elevation of paired CB margins.

H^* and T^* for all CBs are calculated using equations 1&2. This is an important distinction between the works done by Li et al. (2016) and Yu et al. (2017) and our work. Li et al. (2016) and Yu et al. (2017) calculated H^* and T^* for a depositional basin using the depth of the deepest channels observed on the surface of the basin.

RESULTS

Channelized body dimensions

Classification based on the definitions of Gibling (2006) suggest that CBs interpreted in both EQ and LM are either delta distributaries-or meandering channels, with only a small section of these being braided channels (Fig.5). Even though this method creates very sharp boundaries between the different types of CBs, we want to emphasize that in reality these boundaries are gradational. Difference in the types of CBs between the two time periods are only apparent in the upper tails of the distributions. The cumulative distributive functions (CDF) of the widths of CBs from the EQ and LM are similar, spreading over scales of 10^1-10^3 m. However, the EQ distribution contains several CBs that approach widths of 10^4 m (Fig.5). These exceptionally wide EQ CBs are interpreted as paleovalley-fills. The LM strata lacks these exceptionally wide CBs. These wide EQ CBs are also exceptionally thick (Fig.5). The thickness of the CBs from both EQ and LM are between 10^1-10^2 m, except for the wide EQ CBs that are between 10^2-10^3 m thick.

Next, width-to-thickness ratios were calculated for the CBs resolvable in the vertical seismic section (Fig 6). Almost all CBs from EQ have a width-to-depth ratio between 1 to 60, with two being in excess of 100. In comparison, all but one of the LM CBs have width-to-thickness ratios between 1 and 40, with the outlier being 80. The thickest EQ and LM CBs (thicker>100s of m) show low width-to-thickness values (<5) (Fig. 6). The width-to-thickness ratio of the present-day Mississippi river varies between 1 to ~400, but for the portion downstream of the backwater length i.e., till ~300 river kilometers, this ratio is <40 (Blum *et al.*, 2013), which compares well with the width-to-thickness ratios of the LM CBs reported here. The widths of paleovalleys are commonly more than 100 times their thicknesses (Gibling, 2006). That signature can be seen in only two CBs in this dataset, and both of them are from the EQ.

Utilizing the measurements of maximum channel depths and local subsidence rates, H^* and T^* were estimated. We present these measurements in an H^*-T^* space that is divided into four quadrants, based on the values of both the time and depth scales of RSL signal preservation. <5% of the EQ CBs have both H^* and T^* <1, plotting in the signal shredding regime and the rest of the CBs have either $H^*>1$ or both H^* and T^* greater than 1. This suggests that CBs from these time periods have a significant chance of containing signals of changing RSL. The EQ CBs with the lowest H^* and T^* values are interpreted as paleovalleys from their geometries and thus their scales are likely the result of sea level driven allogenic processes. In comparison, ~40 % of the LM CBs plot in the shredding regime, with only one LM CB having $H^*>1$ and 60% of them $T^*>1$. Close to half of the total population of interpreted LM CBs are expected to shred the RSL signal. Further, all of the larger CBs fall in the shredding regime and do not have width and depth statistics indicative of paleovalleys.

To estimate uncertainties in the H^* and T^* estimate, a lower sedimentation rate of 0.26 m/ka (reported by Straub et al. (2009) from the southeastern part of the Mississippi River basin) was used to calculate the same suite of statistics as discussed above (Fig. 7). With the lower sedimentation rate, all but one LM CBs plot in the shredding regime. For the EQ <5% of the CBs plot in the shredding regime, with the rest having $H^*>1$. Almost 95% of the EQ CBs are expected to store the RSL signal in this case.

<u>Present-day Mississippi channel width</u>

The present-day Mississippi river channel and channel belt dimensions are compared with CB's from both the LM and EQ. Only a few of these EQ and LM CBs, which are a collection of channelized sediment transport systems of varying scales, are comparable to the present-day Mississippi-scale system. The important observation is that the thicker and wider CBs present in the EQ make the upper tails of the distributions heavier compared to that of the modern channel, channel-belt or the upper tail from LM (Fig 8). The dimensions of the present-day autogenic Mississippi River channel and channel-belt downstream from the backwater reach are smaller than the dimensions of the interpreted paleovalleys seen in the upper tail of the EQ CBs. The width and the thickness of the EQ features areclose to a factor of two larger than anything seen in the LM distribution and the present-day Mississippi River. Thus, the dimensions of the present-day autogenic Mississippi river channel are closer to those found in the distribution of CB dimensions from the LM (Fig. 8a). This supports an interpretation that the LM strata dominantly stores autogenic process signals, while allogenic RSL signals are likely lacking due to shredding by the autogenic processes. Even though the modern-day Mississippi channel belt width is smaller than the that of the heavier tail of the EQ CBs, the scales of these features are closer in size than that of the present-day Mississippi river (Fig. 8b).

Discussion

The measured (and estimated) width and thickness of CBs from the EQ and LM in the MRD show a wide distribution of scales but differences in dimensions that we interpret to be resulting from different allogenic forcings and the basin's signal preservation potential. For each time period, the *H**-*T** distributions span high values associated with the smaller coastal channels to smaller values tied to CBs with scales similar to the modern-day Mississippi River. The range and period of RSL cycles in the LM were less than many of the resulting CB thicknesses and the times to generate basin wide deposits of equivalent thicknesses as the CBs, as ~50% of these CBs fall in the signal shredding regime. However, this result alone does not fully support the shredding of RSL signals in the LM as 1) half of the CBs in the LM do fall within the signal preservation regime and 2) CBs that fall within the shredding regime could have scales influenced by allogenic signals like RSL change, but these signals are obscured by the scale of the autogenic signals and are not statistically detectable.

In contrast, 95% of the EQ CB's fall within the signal preservation regime of the *H**-*T** plot. This suggests a much higher likelihood that strata of the EQ contain definitive signals of RSL change. Further, of the 5% of EQ CBs that do fall within the shredding regime most have scales more than those found on the modern (autogenic) configuration of the Mississippi River and some have width:thickness ratios that suggest they formed during the filling of paleo-valleys carved in response to changing RSL. These observations support signal preservation of changing RSL in EQ strata. This is in line with our predictions based on signal shredding theory.

We note, though, that all of the mapped CB's in the LM, also have scales that are equal to or less than the scales of the modern day autogenic Mississippi channel. We do acknowledge that if the Mississippi river was smaller due to the lower sediment and/or water flux due to changes in the hinterland, then the autogenic scales of the past channel would have been smaller than the present-day Mississippi river. Taken together, these observations support shredding of signals of RSL change in the LM strata. This is not to disregard the fact that RSL signals might reside in smaller systems akin to the majority of the LM CBs. However, the enhanced scales of width and depth of these smaller systems, as a result of being perturbed by RSL change, might be difficult to identify due to their position within the autogenic distribution of CB dimensions. As we only see the definitive evidence of RSL signal preservation in the larger trunk system, our analysis points to the trunk system setting the fidelity of the larger basin.

The LM CBs are not as wide as the present-day Mississippi channel belt when characterized over its final 800 kms. However, the widest EQ CBs are also narrower than the present-day Mississippi channel belt over this reach. A second comparison focuses on just the lower 300 km of the modern Mississippi River channel belt. This region is within the backwater reach, where channel belts have scales similar to individual channel features, due to the limited lateral migration rates of channels from loss of bedload at the normal-backwater flow transition. We suggest that many of the mapped CBs are individual channel fills, rather than channel-belt fills, given the width-to-depth ratios of features mappable in both time slices and vertical cross-sections. This might indicate that they were deposited in backwater reaches, and thus we should compare their scales to modern channel belt scales in the backwater reach (i.e., lower 300 river kms). The widest EQ CBs are of the same width or slightly wider than the modern channel belt thickness in the lower ~300 km. But these CBs are thicker than either the depth of the present-day Mississippi channel or the thickness of the modern channel belt. Thus, we suggest that there is a high chance of these EQ CBs scales being set by allogenic sea level perturbations, and thus storing RSL signals.

To document and analyze the preservation of RSL signals in stratigraphy, it is useful to estimate paleo-channel dimensions from stratigraphic observables. There are several ways to estimate paleo-channel depths from preserved channel fills, but there can be substantial error associated with these methods (Alexander et al., 2020; Mohrig et al., 2000). Some of this error is associated with the constraints of the data to differentiate stratigraphic products linked to autogenic channel processes from products of allogenic forcing. For example, recent work shows that autogenic processes like avulsions can create backwater and flood scours whose dimensions can be comparable to incised paleovalleys formed in response to changing RSL (Ganti et al., 2019; Trower et al., 2018).

The paleovalleys reported in this study are not as wide as is commonly expected for systems comparable to the Mississippi River. The width to thickness ratio as well as the width of the CBs identified as paleovalleys are in the lower end of the range of dimensions suggested by Gibling (2006), which are only slightly wider than the modern-day channel belt dimensions. These paleovalleys are thicker than the average Gulf of Mexico paleovalleys from the last glaciation (Anderson *et al.*, 2016). The width of a paleovalley depend on the number of the channel-belt sandbodies contained in it and their individual widths (Blum *et al.*, 2013). The widest paleovalleys seen here are composed of only a few individual sand bodies whose thickness are in the order of 10^1 m, thus restricting the width of the paleovalleys itself (Fig. 3). There can be a number of reasons behind including the sediment flux, the amount of relative sea-level change, the shelf morphology as well as the differences in the basal valley-fill surface (Törnqvist *et al.*, 2006; Blum *et al.*, 2013). However, the aim of this work is to test the signal shredding theory in a relatively small area with field data, and the absence of larger paleovalleys can be restricted by the size of the seismic volume, which would obstruct us from mapping larger CBs. For future work, the geographic scale of exploration related to the signal shredding theory can be a probable avenue to explore.

The interpreted paleovalleys from the EQ stratigraphy plot in the signal shredding domain, which probably carry the signals of RSL change (Fig. 7). These geobodies were likely constructed by channels of significant size that were further incised by allogenic RSL change. Channels on the upper end of the autogenic spectrum that responded to large RSL change create the most easily identifiable signal of paleo RSL-change. This contrasts with other smaller-scale channels that were already well within the autogenic band, that when tugged by RSL change deepened and widened, but not out of the autogenic bands. The predicted changes in deposition from proximal to distal parts of the system cannot be conclusively tested in this work, due to the limited geographical region explored, and the limited well-log data from the EQ time-period, which could aid identification of grain size signals in the strata. These CBs are conduits of sediment transport to the continental shelf and in time, to the deep marine realm. The competition between the allogenic and autogenic processes during changing RSL cycles on them must have consequences for sediment transport as well. Future work can be focused on this issue as well as other sub-seismic scale observations.

CONCLUSIONS

This work demonstrates how to apply signal shredding theory to field scale settings. Even though a number of numerical and physical experiments have explored signal shredding of RSL change, changing sediment or fluid flux (Jerolmack and Paola, 2010; Li et al., 2016; von der Heydt et al., 2003; Yu et al., 2017), this is the first test of this idea at field scale. While we cannot definitively state that signals of RSL change are present or not in either of the two time periods explored, broadly speaking the results support the stratigraphic signal shredding framework for RSL cycles. This supports the premise that in some sedimentary basins, some RSL cycles are of insufficient duration or magnitude to produce stratigraphic products outside the range of the products of autogenic channel dynamics. It highlights the need for multiple hypotheses and scenario development that should be considered when interpreting stratal architecture, scales, and geometries for interpretation of global RSL changes.

ACKNOWLEDMENTS

This study was supported by the National Science Foundation (grant EAR-1424312). We also acknowledge Dr. Zoltan Sylvester for the python script for calculation of CB dimensions, and Dr. David Mohrig and Dr. Torbjörn Törnqvist for discussions and valuable suggestions. (We will add the reviewers as well).

FIGURE CAPTIONS

Figure 1: a) Map of the study area. The red line is the extent of the continental shelf edge during the Early Quaternary, while the black line is the location of the shelf-edge during the Late Miocene. The study area was inbound of the shelf edge during both times. b) Age vs sediment thickness for Well API # 177094078100 in the study region. Age data was determined for biostratigraphic markers and best-fit trend line gives a long-term sedimentation or subsidence rate of 0.54 m/ka. The planktonic microfossils were recovered from well API#177094078100, with data made publicly available by United States Department of the Interior Bureau of Ocean Energy Management.

Figure 2: A dip section showing the two-way travel time and depth relationship with respect to the relative sea level history adapted from Miller et al. (2005). The blue star shows the presence of an Early Quaternary, EQ, microfossil which is used to constrain the time-period of interest in

the EQ. The specific window of EQ strata analyzed is demarcated by the colored box labeled Early Quaternary. The Late Miocene, LM, stratigraphy has been constrained from foraminifera samples, shown by a yellow star, which constrains the age of the time period of interest right below, shown by the colored box labeled Late Miocene. Examples of CBs interpreted in the vertical sections for both EQ and LM are shown. The white dashed line shows the approximate location of the time slice shown in Fig. 1a as an example of EQ stratigraphy and the black dashed line is the same shown in fig 4 for Late Miocene.

Figure 4: A variance time-slice (600 ms) from EQ time-period. Panel A shows the uninterpreted section and Panel B shows the interpreted CBs in yellow. Panel C shows an example of an interpreted paleovalley.

Figure 5: shows a variance time-slice from the LM time-period. Panel A shows the uninterpreted section and Panel B shows the interpreted CBs in yellow.

Figure 6: A comparison of CB widths and thicknesses for Early Quaternary (shown by circles) and Late Miocene (shown by crosses). The left hand panel shows the cumulative distribution function, CDF, of the CB widths, and the right hand panel shows the CDF of the CB thickness. In both cases, the distributions are similar for two time periods with the exception of the largest CB features. The Early Quaternary has a pronounced heavy tail signifying presence of paleovalleys, meaning the EQ stratigraphy preserved the RSL signal. We have used a median

value for calculating the different types of channelized bodies in this figure, but we acknowledge that these boundaries are gradational in reality.

Figure 7: The cumulative distribution function of the width-to-thickness ratio of the EQ (shown by circles) and LM (shown by crosses) CBs. CBs are colored according to their thickness.

Figure 8: H* and T* cross plot for CBs of the EQ (shown by circles) and LM (shown by crosses) calculated with two sedimentation rates. The area where H* and T* are less than 1 is the shredding regime and the rest of the space is the preservation regime. Symbols are colored by their distribution CDF values, shown in the colorbar. The shaded area in red shows the uncertainty band where the calculated H* and T* values can lie with varying input values.

Figure 9: Comparing CB widths and thicknesses between the EQ (shown by circles), LM (shown by crosses), and the present-day Mississippi river channel (shown by triangles) and CB (shown by diamonds) width and depth. The cumulative distribution function of the CB, a) channel and b) channel body widths. c) CDF of CB, channel and channel body thickness. In both cases, a difference is noted in the positive tail of the distributions, with more weight found in the EQ heavy tail.

TABLE CAPTIONS

Table 1: The dimensions and their ratio used in the analysis to interpret types of channelized bodies and calculate their thickness, following Gibling (2006).

FIGURES

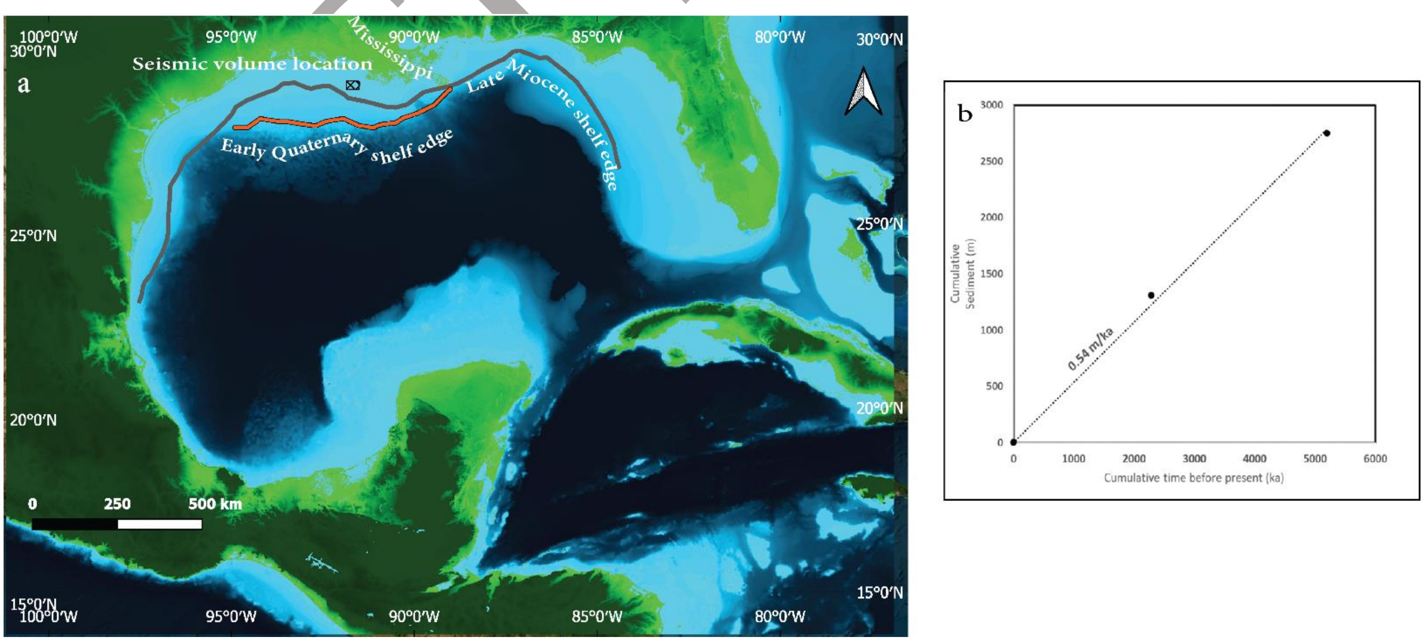

FIGURE 1

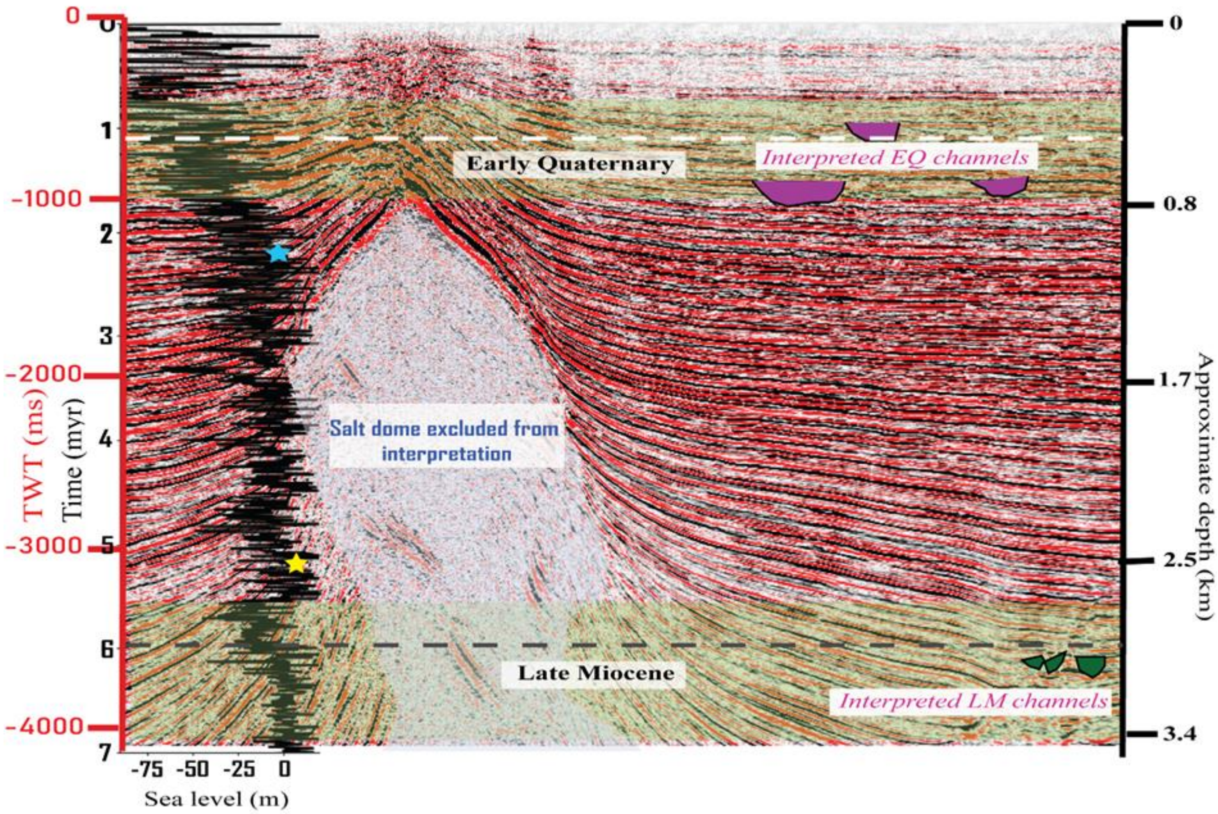

0
1
-1000
2
3
-2000
4
-3000
5
6
-4000
7
TWT (ms)
Time (myr)
-75 -50 -25 0
Sea level (m)
Early Quaternary
Interpreted EQ channels
Salt dome excluded from interpretation
Late Miocene
Interpreted LM channels
0
0.8
1.7
2.5
3.4
Approximate depth (km)

FIGURE 2

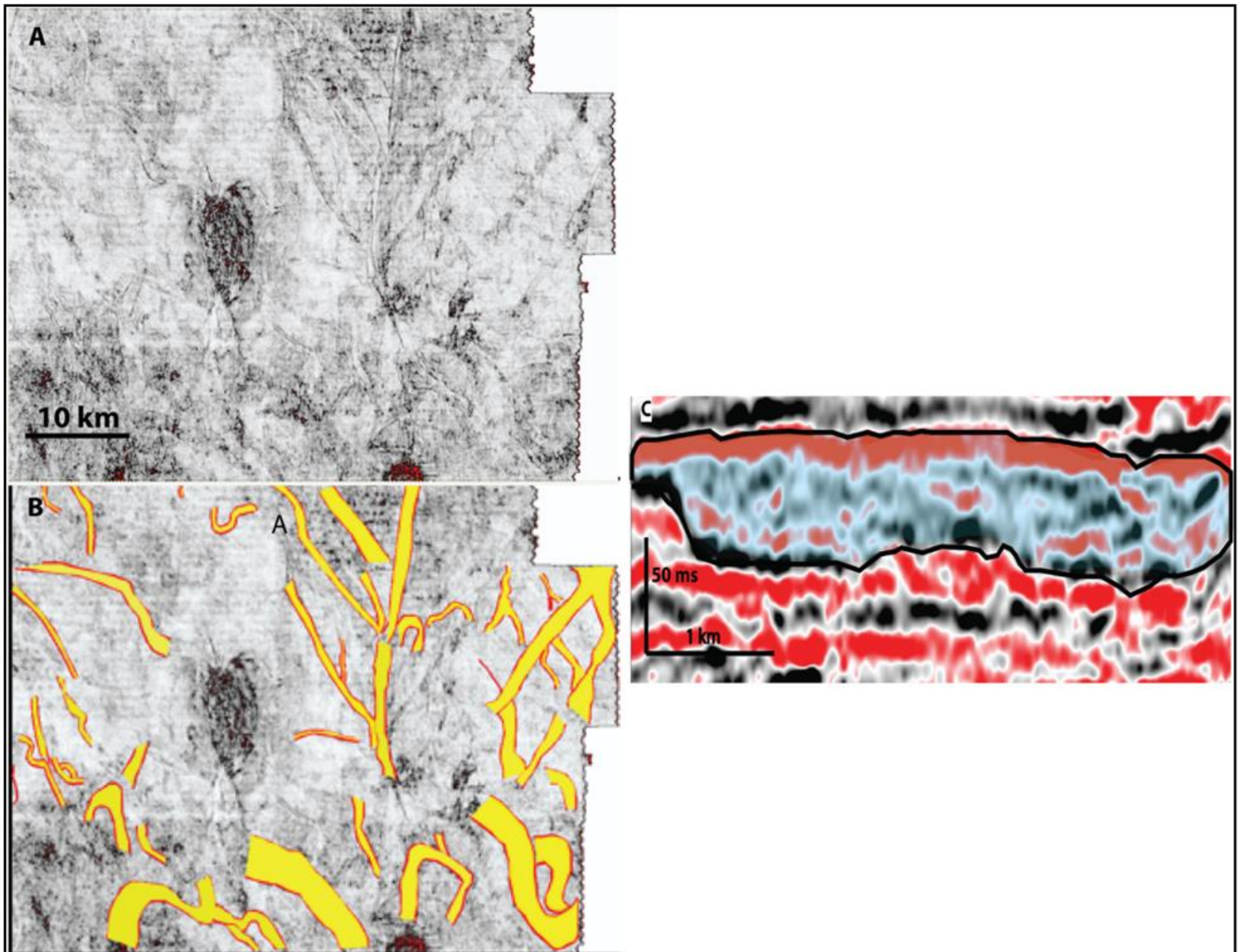

FIGURE 3

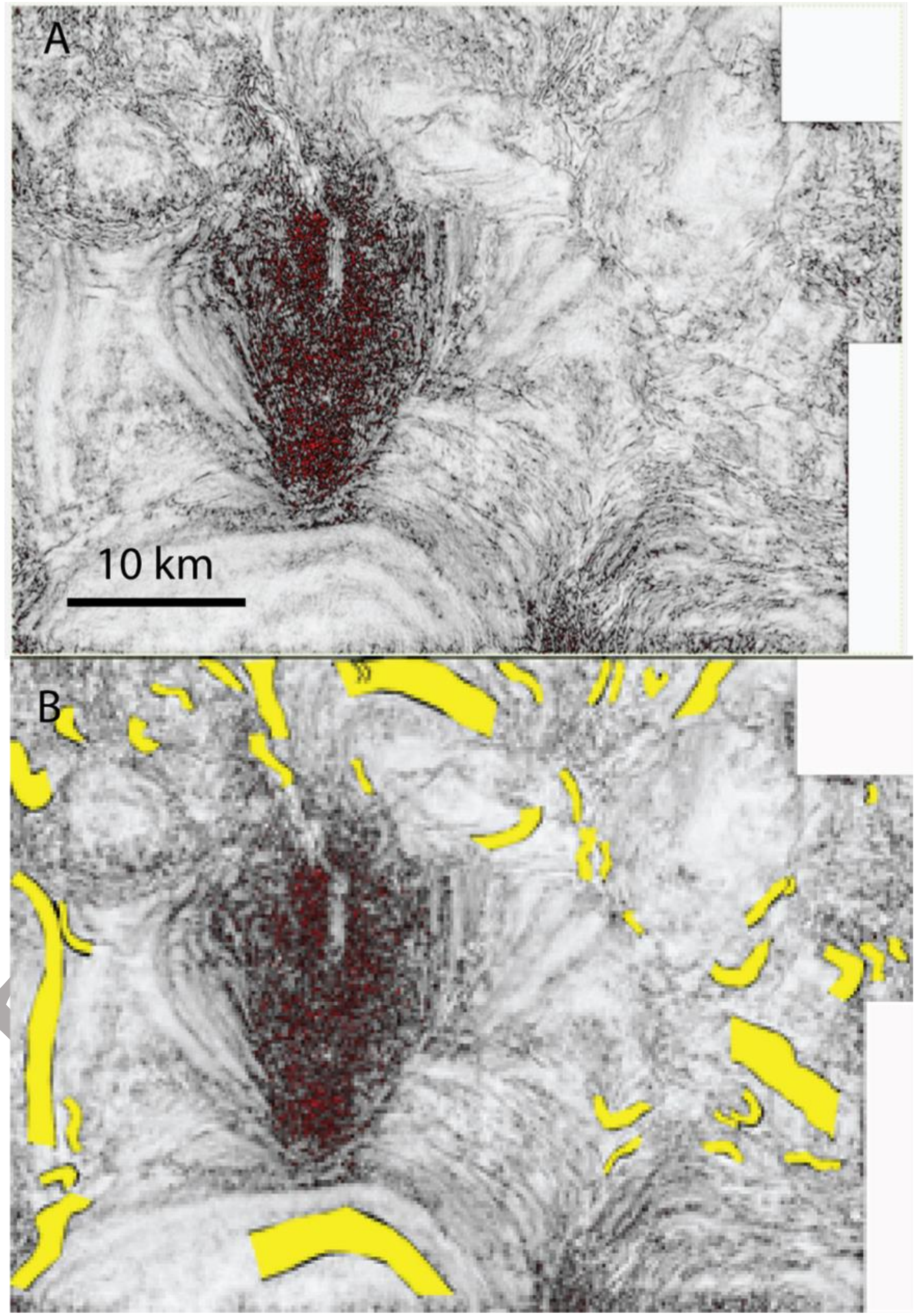

FIGURE 4

8

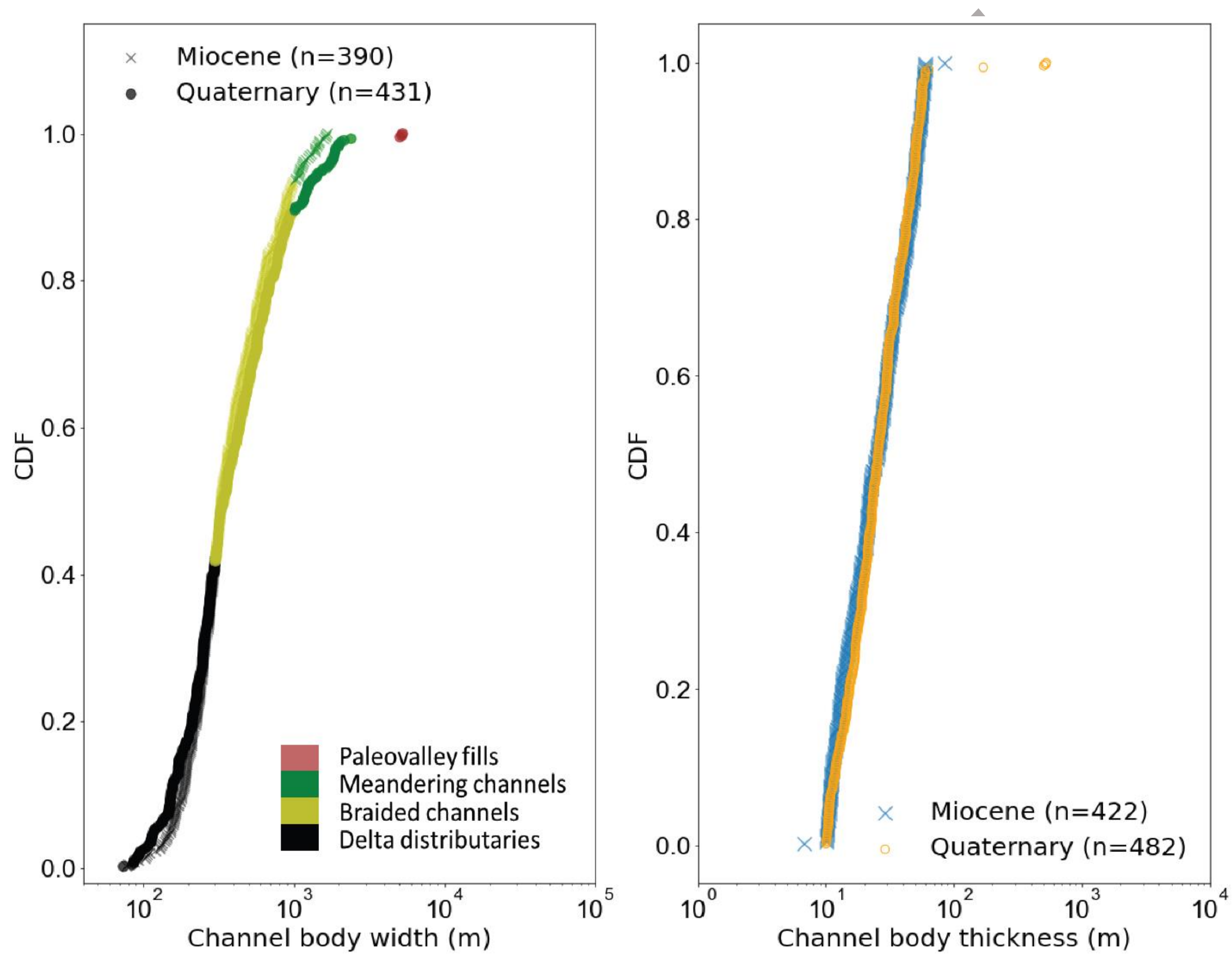
Miocene (n=390)
Quaternary (n=431)
1.0
0.8
0.6
0.4
0.2
0.0
CDF
Paleovalley fills
Meandering channels
Braided channels
Delta distributaries
10^2
10^3
10^4
10^5
Channel body width (m)
1.0
0.8
0.6
0.4
0.2
0.0
CDF
Miocene (n=422)
Quaternary (n=482)
10^0
10^1
10^2
10^3
10^4
Channel body thickness (m)

FIGURE 5

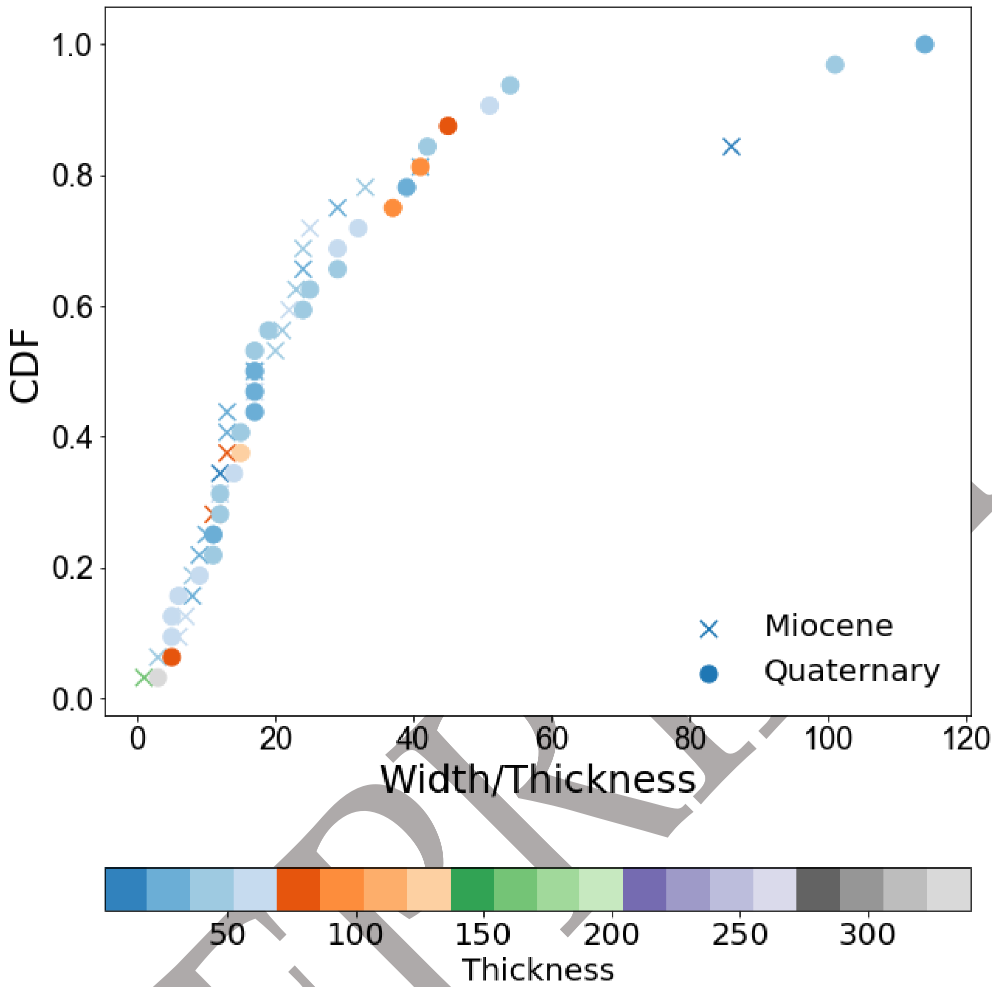

590

591

592 **FIGURE 6**

593

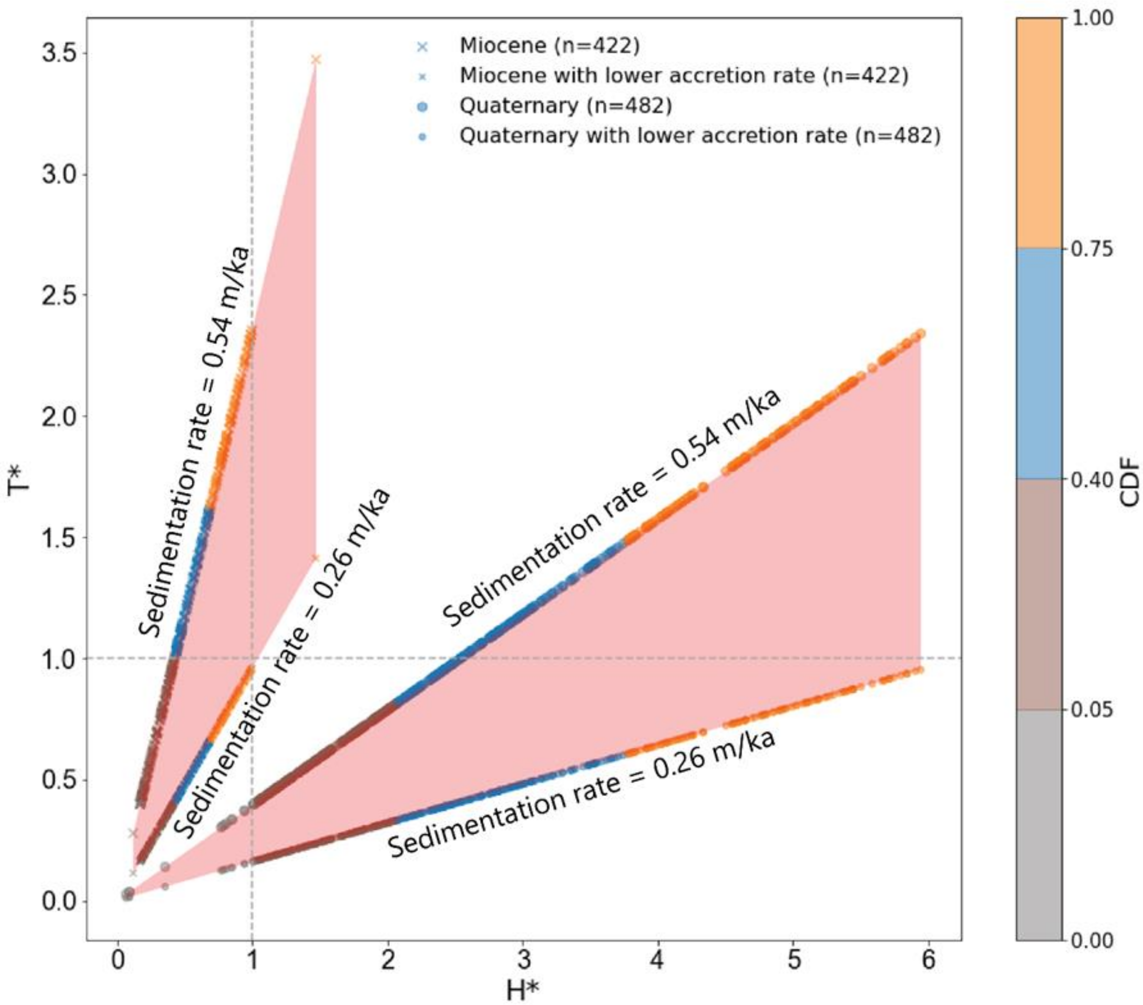
Miocene (n=422)
Miocene with lower accretion rate (n=422)
Quaternary (n=482)
Quaternary with lower accretion rate (n=482)
Sedimentation rate = 0.54 m/ka
Sedimentation rate = 0.26 m/ka
Sedimentation rate = 0.54 m/ka
Sedimentation rate = 0.26 m/ka
T*
H*
CDF
0.0
0.5
1.0
1.5
2.0
2.5
3.0
3.5
0
1
2
3
4
5
6
0.00
0.05
0.40
0.75
1.00

FIGURE 7

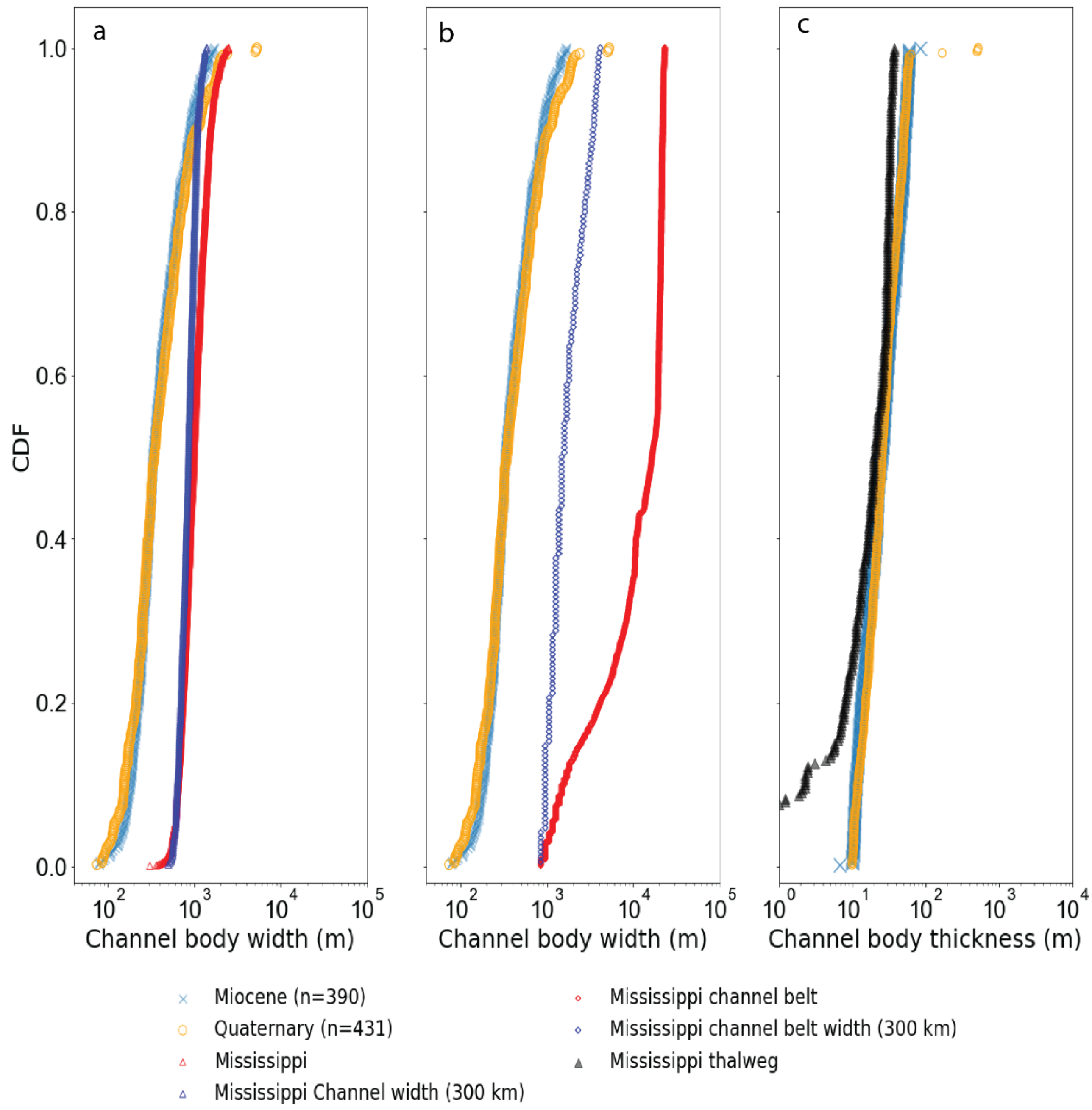
a
b
c
CDF
1.0
0.8
0.6
0.4
0.2
0.0
Channel body width (m)
Channel body width (m)
Channel body thickness (m)
Miocene (n=390)
Quaternary (n=431)
Mississippi
Mississippi Channel width (300 km)
Mississippi channel belt
Mississippi channel belt width (300 km)
Mississippi thalweg

FIGURE 8

TABLES

Types of channel	Common range for width (km)	Maximum Width to Depth ratio
Delta Distributaries	0.01-0.3	1:5
Meandering	0.3-3	1:30
Braided/Low-Sinuosity rivers	0.5-10	1:50
Valleys fills within alluvial and marine strata	0.2-25	1:10

TABLE 1

REFERENCES

Akers, W., 1955, Some planktonic foraminifera of the American Gulf Coast and suggested correlations with the Caribbean Tertiary: Journal of Paleontology, p. 647-664.

Alexander, J. S., McElroy, B. J., Huzurbazar, S., and Murr, M. L., 2020, Elevation gaps in fluvial sandbar deposition and their implications for paleodepth estimation: Geology, v. 48, no. 7, p. 718-722.

Alley, R. B., Clark, P. U., Huybrechts, P., and Joughin, I., 2005, Ice-sheet and sea-level changes: science, v. 310, no. 5747, p. 456-460.

Anderson, J. B., Rodriguez, A., Abdulah, K. C., Fillon, R. H., Banfield, L. A., Mckeown, H. A., and Wellner, J. S., 2004, Late Quaternary stratigraphic evolution of the northern Gulf of Mexico margin: a synthesis: SEPM Special Publication, v. 79, p. 1-23.

Anderson, J. B., Wallace, D. J., Simms, A. R., Rodriguez, A. B., Weight, R. W., and Taha, Z. P., 2016, Recycling sediments between source and sink during a eustatic cycle: Systems of late Quaternary northwestern Gulf of Mexico Basin: Earth-science reviews, v. 153, p. 111-138.

Armitage, J. J., Burgess, P. M., Hampson, G. J., and Allen, P. A., 2018, Deciphering the origin of cyclical gravel front and shoreline progradation and retrogradation in the stratigraphic record: Basin Research, v. 30, p. 15-35.

Bentley Sr, S., Blum, M., Maloney, J., Pond, L., and Paulsell, R., 2016, The Mississippi River source-to-sink system: Perspectives on tectonic, climatic, and anthropogenic influences, Miocene to Anthropocene: Earth-Science Reviews, v. 153, p. 139-174.

Best, J. L., and Ashworth, P. J., 1997, Scour in large braided rivers and the recognition of sequence stratigraphic boundaries: Nature, v. 387, no. 6630, p. 275-277.

Bhattacharya, J. P., 2011, Practical problems in the application of the sequence stratigraphic method and key surfaces: integrating observations from ancient fluvial-deltaic wedges with Quaternary and modelling studies: Sedimentology, v. 58, no. 1, p. 120-169.

Blum, M., 2019, Organization and reorganization of drainage and sediment routing through time: The Mississippi River system: Geological Society, London, Special Publications, v. 488, no. 1, p. 15-45.

Blum, M., Martin, J., Milliken, K., and Garvin, M., 2013, Paleovalley systems: Insights from Quaternary analogs and experiments: Earth-Science Reviews, v. 116, p. 128-169.

Blum, M., and Pecha, M., 2014, Mid-Cretaceous to Paleocene North American drainage reorganization from detrital zircons: Geology, v. 42, no. 7, p. 607-610.

Blum, M. D., Hattier-Womack, J., Kneller, B., Martinsen, O., and McCaffrey, B., 2009, Climate change, sea-level change, and fluvial sediment supply to deepwater depositional systems: External Controls on Deep Water Depositional Systems: SEPM, Special Publication, v. 92, p. 15-39.

Blum, M. D., Milliken, K. T., Pecha, M. A., Snedden, J. W., Frederick, B. C., and Galloway, W. E., 2017, Detrital-zircon records of Cenomanian, Paleocene, and Oligocene Gulf of Mexico drainage integration and sediment routing: Implications for scales of basin-floor fans: Geosphere, v. 13, no. 6, p. 2169-2205.

Blum, M. D., and Price, D. M., 1998, Quaternary alluvial plain construction in response to glacio-eustatic and climatic controls, Texas Gulf coastal plain.

Burgess, P. M., and Prince, G. D., 2015, Non-unique stratal geometries: implications for sequence stratigraphic interpretations: Basin Research, v. 27, no. 3, p. 351-365.

Burgess, P. M., Steel, R. J., Granjeon, D., Hampson, G., and Dalrymple, R., 2008, Stratigraphic forward modeling of basin-margin clinoform systems: Implications for controls on topset and shelf width and timing of formation of shelf-edge deltas: Recent advances in models of siliciclastic shallow-marine stratigraphy, v. 90, p. 35-45.

Buzas-Stephens, P., Livsey, D. N., Simms, A. R., and Buzas, M. A., 2014, Estuarine foraminifera record Holocene stratigraphic changes and Holocene climate changes in ENSO and the North American monsoon: Baffin Bay, Texas: Palaeogeography, Palaeoclimatology, Palaeoecology, v. 404, p. 44-56.

Catuneanu, O., Abreu, V., Bhattacharya, J. P., Blum, M. D., Dalrymple, R. W., Eriksson, P. G., Fielding, C. R., Fisher, W. L., Galloway, W. E., Gibling, M. R., Giles, K. A., Holbrook, J. M., Jordan, R., Kendall, C. G. S. C., Macurda, B., Martinsen, O. J., Miall, A. D., Neal, J. E., Nummedal, D., Pomar, L., Posamentier, H. W., Pratt, B. R., Sarg, J. F., Shanley, K. W., Steel, R. J., Strasser, A., Tucker, M. E., and Winker, C., 2009a, Towards the standardization of sequence stratigraphy: Earth-Science Reviews, v. 92, no. 1, p. 1-33.

—, 2009b, Towards the standardization of sequence stratigraphy: Earth-Science Reviews, v. 92, p. 1-33.

Chapin, C. E., 2008, Interplay of oceanographic and paleoclimate events with tectonism during middle to late Miocene sedimentation across the southwestern USA: Geosphere, v. 4, no. 6, p. 976-991.

Ciarletta, D. J., Lorenzo-Trueba, J., and Ashton, A., 2019, Mechanism for retreating barriers to autogenically form periodic deposits on continental shelves: Geology, v. 47, no. 3, p. 239-242.

Clark, P. U., McCabe, A. M., Mix, A. C., and Weaver, A. J., 2004, Rapid rise of sea level 19,000 years ago and its global implications: Science, v. 304, no. 5674, p. 1141-1144.

Combellas-Bigott, R. I., and Galloway, W. E., 2006, Depositional and structural evolution of the middle Miocene depositional episode, east-central Gulf of Mexico: AAPG bulletin, v. 90, no. 3, p. 335-362.

Diegel, F. A., Karlo, J., Schuster, D., Shoup, R., and Tauvers, P., 1995, Cenozoic structural evolution and tectono-stratigraphic framework of the northern Gulf Coast continental margin: in M. P. A. Jackson, D. G. Roberts, and S. Snelson, eds.,
Salt tectonics: a global perspective: AAPG Memoir, v. 65, p. 109-151.

Fairbanks, R. G., 1989, A 17,000-year glacio-eustatic sea level record: influence of glacial melting rates on the Younger Dryas event and deep-ocean circulation: Nature, v. 342, no. 6250, p. 637-642.

Feeley, M., Moore Jr, T., Loutit, T., and Bryant, W., 1990, Sequence stratigraphy of Mississippi Fan related to oxygen isotope sea level index: AAPG bulletin, v. 74, no. 4, p. 407-424.

Fisk, H. N., and McFarlan Jr, E., 1955, Late Quaternary deltaic deposits of the Mississippi River: Geological Society of America Special Paper, v. 62, p. 279-302.

Frederick, B. C., Blum, M., Fillon, R., and Roberts, H., 2019, Resolving the contributing factors to Mississippi Delta subsidence: Past and Present: Basin Research, v. 31, no. 1, p. 171-190.

Galloway, W. E., 1989, Genetic stratigraphic sequences in basin analysis II: application to northwest Gulf of Mexico Cenozoic basin: AAPG Bulletin, v. 73, no. 2, p. 143-154.

—, 2008, Depositional evolution of the Gulf of Mexico sedimentary basin: Sedimentary basins of the world, v. 5, p. 505-549.

Galloway, W. E., Ganey-Curry, P. E., Li, X., and Buffler, R. T., 2000, Cenozoic depositional history of the Gulf of Mexico basin: AAPG Bulletin, v. 84, no. 11, p. 1743-1774.

Galloway, W. E., Whiteaker, T. L., and Ganey-Curry, P., 2011, History of Cenozoic North American drainage basin evolution, sediment yield, and accumulation in the Gulf of Mexico basin: Geosphere, v. 7, no. 4, p. 938-973.

Ganti, V., Chu, Z., Lamb, M. P., Nittrouer, J. A., and Parker, G., 2014, Testing morphodynamic controls on the location and frequency of river avulsions on fans versus deltas: Huanghe (Yellow River), China: Geophysical Research Letters, v. 41, no. 22, p. 7882-7890.

Ganti, V., Lamb, M. P., and Chadwick, A. J., 2019, Autogenic Erosional Surfaces in Fluvio-deltaic Stratigraphy from Floods, Avulsions, and Backwater Hydrodynamics: Journal of Sedimentary Research, v. 89, no. 8, p. 815-832.

Gibling, M. R., 2006, Width and thickness of fluvial channel bodies and valley fills in the geological record: a literature compilation and classification: Journal of Sedimentary Research, v. 76, p. 731-770.

Gibling, M. R., Fielding, C. R., and Sinha, R., 2011, Alluvial valleys and alluvial sequences: towards a geomorphic assesment, *in* North, C. P., ed., From Rivers to Rock: Geological Society of London Special Publication.

Haq, B. U., 1991, Sequence stratigraphy, sea-level change, and significance for the deep sea: Sedimentation, Tectonics and Eustasy: Sea-Level Changes at Active Margins, p. 1-39.

Haq, B. U., Hardenbol, J., and Vail, P. R., 1987, Chronology of fluctuating sea levels since the Triassic: Science, v. 235, no. 4793, p. 1156-1167.

Harris, A. D., Baumgardner, S. E., Sun, T., and Granjeon, D., 2018, A Poor Relationship Between Sea Level and Deep-Water Sand Delivery: Sedimentary Geology, v. 370, p. 42-51.

Harris, A. D., Covault, J. A., Madof, A. S., Sun, T., Sylvester, Z., and Granjeon, D., 2016, Three-Dimensional Numerical Modeling of Eustatic Control On Continental-Margin Sand DistributionA. D. HARRIS ET AL. NUMERICAL MODELING OF EUSTATIC CONTROL ON CONTINENTAL-MARGIN SAND DISTRIBUTION: Journal of Sedimentary Research, v. 86, no. 12, p. 1434-1443.

Imbrie, J., and Imbrie, J. Z., 1980, Modeling the climatic response to orbital variations: Science, v. 207, no. 4434, p. 943-953.

Jerolmack, D. J., and Paola, C., 2010, Shredding of environmental signals by sediment transport: Geophysical Research Letters, v. 37, p. L19401.

Kim, W., Paola, C., Martin, J., Perlmutter, M. A., and Tapaha, F., 2009, Net pumping of sediment into deep water due to base-level cycling: Experimental and theoretical results, *in* Kneller, B., Martinsen, O. J., and McCaffrey, B., eds., External Controls on Deep-Water Depositional Systems: SEPM Special Publication 92, p. 41-56.

Kim, Y., Kim, W., Cheong, D., Muto, T., and Pyles, D. R., 2013, Piping coarse-grained sediment to a deep water fan through a shelf-edge delta bypass channel: Tank experiments: Journal of Geophysical Research: Earth Surface, v. 118, no. 4, p. 2279-2291.

Krynine, P. D., 1948, The megascopic study and field classification of sedimentary rocks: The Journal of Geology, v. 56, no. 2, p. 130-165.

Li, Q., Yu, L., and Straub, K. M., 2016, Storage thresholds for relative sea-level signals in the stratigraphic record: Geology, v. 44, no. 3, p. 179-182.

Licciardi, J. M., Clark, P. U., Jenson, J. W., and Macayeal, D. R., 1998, Deglaciation of a soft-bedded Laurentide Ice Sheet: Quaternary Science Reviews, v. 17, no. 4-5, p. 427-448.

Lisiecki, L. E., and Raymo, M. E., 2005, A Pliocene-Pleistocene stack of 57 globally distributed benthic delta O-18 records (vol 20, art no PA1003, 2005): Paleoceanography, v. 20, no. 2.

McMillan, M. E., Heller, P. L., and Wing, S. L., 2006, History and causes of post-Laramide relief in the Rocky Mountain orogenic plateau: Geological Society of America Bulletin, v. 118, no. 3-4, p. 393-405.

Miller, K. G., Kominz, M. A., Browning, J. V., Wright, J. D., Mountain, G. S., Katz, M. E., Sugarman, P. J., Cramer, B. S., Christie-Blick, N., and Pekar, S. F., 2005, The phanerozoic record of global sea-level change: Science, v. 310, no. 5752, p. 1293-1298.

Mohrig, D., Heller, P. L., Paola, C., and Lyons, W. J., 2000, Interpreting avulsion process from ancient alluvial sequences: Guadalope-Matarranya (northern Spain) and Wasatch Formation (western Colorado): Geoogical Society of America Bulletin, v. 112, p. 1787-1803.

Nittrouer, J. A., 2013, Backwater hydrodynamics and sediment transport in the lowermost Mississippi River Delta: Implications for the development of fluvial-deltaic landforms in a large lowland river: IAHS-AISH Publ, v. 358, p. 48-61.

Nittrouer, J. A., Shaw, J., Lamb, M. P., and Mohrig, D., 2012, Spatial and temporal trends for water-flow velocity and bed-material sediment transport in the lower Mississippi River: Geological Society of America Bulletin, v. 124, no. 3-4, p. 400-414.

Olariu, C., and Steel, R. J., 2009, Influence of point-source sediment-supply on modern shelf-slope morphology: Implications for interpretation of ancient shelf margins: Basin Research, v. 21, no. 5, p. 484-501.

Paola, C., 2000, Quantitative models of sedimentary basin filling: Sedimentology, v. 47, p. 121-178.

Paola, C., Ganti, V., Mohrig, D., Runkel, A. C., and Straub, K. M., 2018, Time Not Our Time: Physical Controls on the Preservation and Measurement of Geologic Time: Annual Review of Earth and Planetary Sciences, v. 46, p. 409-438.

Peel, F., Travis, C., and Hossack, J., 1995, Genetic structural provinces and salt tectonics of the Cenozoic offshore US Gulf of Mexico: A preliminary analysis: in M. P. A. Jackson, D. G. Roberts, and S. Snelson, eds., Salt tectonics: a global perspective:AAPG Memoir, v. 65, p. 153-175.

Peel, F. J., 2014, How do salt withdrawal minibasins form? Insights from forward modelling, and implications for hydrocarbon migration: Tectonophysics, v. 630, p. 222-235.

Pettijohn, F., Potter, P., and Siever, R., 1972, Sand and Sandstone. Springer-Verlag, Berlin Heidelberg New York.

Posamentier, H. W., and Vail, P. R., 1988a, Eustatic controls on clastic deposition II - sequence and systems tract models, *in* Wilgus, C. K., Hastings, B. S., Posamentier, H. P., Van Wagoner, J. V., Ross, C. A., and Kendall, C. G. S. C., eds., Sea-Level Changes, SEPM special publicaiton 42, p. 125-154.

—, 1988b, Eustatic Controls on Clastic Deposition II—sequence and Systems Tract Models: SEPM Special Publications, p. 125-154.

Raymo, M. E., Lisiecki, L., and Nisancioglu, K. H., 2006, Plio-Pleistocene ice volume, Antarctic climate, and the global δ18O record: Science, v. 313, no. 5786, p. 492-495.

Romans, B. W., Castelltort, S., Covault, J. A., Fildani, A., and Walsh, J., 2016, Environmental signal propagation in sedimentary systems across timescales: Earth-Science Reviews, v. 153, p. 7-29.

Sadler, P. M., 1981, Sediment accumulation rates and the completeness of stratigraphic sections: Journal of Geology, v. 89, p. 569-584.

Saucier, R. T., 1994, Geomorphology and Quaternary geologic history of the Lower Mississippi Valley, US Army Engineer Waterways Experiment Station.

Simms, A. R., Anderson, J. B., DeWitt, R., Lambeck, K., and Purcell, A., 2013, Quantifying rates of coastal subsidence since the last interglacial and the role of sediment loading: Global and planetary change, v. 111, p. 296-308.

Strong, N., and Paola, C., 2008, Valleys that never were: time surfaces versus stratigraphic surfaces: Journal of Sedimentary Research, v. 78, no. 7-8, p. 579-593.

Swartz, J. M., Cardenas, B. T., Mohrig, D., and Passalacqua, P., 2022, Tributary channel networks formed by depositional processes: Nature Geoscience, v. 15, no. 3, p. 216-221.

Sylvester, Z., Durkin, P., Hubbard, S., and Mohrig, D., 2021, Autogenic translation and counter point bar deposition in meandering rivers: GSA Bulletin.

Toby, S. C., Duller, R. A., De Angelis, S., and Straub, K. M., 2019, A stratigraphic framework for the preservation and shredding of environmental signals: Geophysical Research Letters.

Tofelde, S., Savi, S., Wickert, A. D., Bufe, A., and Schildgen, T. F., 2019, Alluvial channel response to environmental perturbations: fill-terrace formation and sediment-signal disruption: Earth Surface Dynamics, v. 7, no. 2, p. 609-631.

Trampush, S., Hajek, E., Straub, K., and Chamberlin, E., 2017, Identifying autogenic sedimentation in fluvial-deltaic stratigraphy: Evaluating the effect of outcrop-quality data on the compensation statistic: Journal of Geophysical Research-Earth Surface, v. 122, p. 1-23.

Trampush, S. M., and Hajek, E. A., 2017, Preserving proxy records in dynamic landscapes: Modeling and examples from the Paleocene-Eocene Thermal Maximum: Geology, v. 45, no. 11, p. 967-970.

Trower, E. J., Ganti, V., Fischer, W. W., and Lamb, M. P., 2018, Erosional surfaces in the Upper Cretaceous Castlegate Sandstone (Utah, USA): Sequence boundaries or autogenic scour from backwater hydrodynamics?: Geology, v. 46, no. 8, p. 707-710.

Van De Wiel, M. J., and Coulthard, T. J., 2010, Self-organized criticality in river basins: Challenging sedimentary records of environmental change: Geology, v. 38, no. 1, p. 87-90.

Van Wagoner, J., Posamentier, H., Mitchum, R., Vail, P., Sarg, J., Loutit, T., and Hardenbol, J., 1988, An overview of the fundamentals of sequence stratigraphy and key definitions.

Van Wagoner, J. C., 1995, Sequence stratigraphy and marine to nonmarine facies architecture of foreland basin strata, Book Cliffs, Utah, U.S.A., *in* Van Wagoner, J. C., and Bertram, G. T., eds., Sequence Stratigraphy of Foreland Basin Deposits: Outcrop and Subsurface Examples from the Createaceous of North America, Volume 64, American Association of Petroleum Geologists, Memoirs, p. 137-223.

von der Heydt, A., Grossmann, S., and Lohse, D., 2003, Response maxima in modulated turbulence. II. Numerical simulations: Physical Review E, v. 68, no. 6, p. 066302.

Wang, Y., Straub, K. M., and Hajek, E. A., 2011, Scale-dependent compensational stacking: An estimate of autogenic time scales in channelized sedimentary deposits: Geology, v. 39, no. 9, p. 811-814.

Weimer, P., 1991, Sequence stratigraphy of the Mississippi Fan related to oxygen isotope sea level index: discussion: AAPG Bulletin, v. 75, no. 9, p. 1500-1507.

Winker, C. D., 1982, Cenozoic shelf margins, northwestern Gulf of Mexico.

Wolstencroft, M., Shen, Z., Törnqvist, T. E., Milne, G. A., and Kulp, M., 2014, Understanding subsidence in the Mississippi Delta region due to sediment, ice, and ocean loading: Insights from geophysical modeling: Journal of Geophysical Research: Solid Earth, v. 119, no. 4, p. 3838-3856.

Wu, X., 2004, Upper Miocene depositional history of the central Gulf of Mexico Basin, The University of Texas at Austin.

Xu, J., Snedden, J. W., Galloway, W. E., Milliken, K. T., and Blum, M. D., 2017, Channel-belt scaling relationship and application to early Miocene source-to-sink systems in the Gulf of Mexico basin: Geosphere, v. 13, no. 1, p. 179-200.

Yu, L., Li, Q., and Straub, K. M., 2017, Scaling the Response of Deltas To Relative-Sea-Level Cycles By Autogenic Space and Time Scales: A Laboratory Study: Journal of Sedimentary Research, v. 87, no. 8, p. 817-837.

Zachos, J., Pagani, M., Sloan, L., Thomas, E., and Billups, K., 2001, Trends, rhythms, and aberrations in global climate 65 Ma to present: science, v. 292, no. 5517, p. 686-693.

Catuneanu, O., Abreu, V., Bhattacharya, J. P., Blum, M. D., Dalrymple, R. W., Eriksson, P. G., Fielding, C. R., Fisher, W. L., Galloway, W. E., Gibling, M. R., Giles, K. A., Holbrook, J. M., Jordan, R., Kendall, C. G. S. C., Macurda, B., Martinsen, O. J., Miall, A. D., Neal, J. E., Nummedal, D., Pomar, L., Posamentier, H. W., Pratt, B. R., Sarg, J. F., Shanley, K. W., Steel, R. J., Strasser, A., Tucker, M. E., and Winker, C., 2009, Towards the standardization of sequence stratigraphy: Earth-Science Reviews, v. 92, no. 1, p. 1-33.

Fernandes, A. M., Törnqvist, T. E., Straub, K. M., and Mohrig, D., 2016, Connecting the backwater hydraulics of coastal rivers to fluvio-deltaic sedimentology and stratigraphy: Geology, v. 44, no. 12, p. 979-982.

Jerolmack, D. J., and Paola, C., 2010, Shredding of environmental signals by sediment transport: Geophysical Research Letters, v. 37, p. L19401.

Leopold, L. B., and Wolman, M. G., 1960, River Meanders: Geological Society of America Bulletin, v. 71, no. 6, p. 769-793.

Li, Q., Yu, L., and Straub, K. M., 2016, Storage thresholds for relative sea-level signals in the stratigraphic record: Geology, v. 44, no. 3, p. 179-182.

Lisiecki, L. E., and Raymo, M. E., 2005, A Pliocene-Pleistocene stack of 57 globally distributed benthic delta O-18 records (vol 20, art no PA1003, 2005): Paleoceanography, v. 20, no. 2.

Miller, K. G., Kominz, M. A., Browning, J. V., Wright, J. D., Mountain, G. S., Katz, M. E., Sugarman, P. J., Cramer, B. S., Christie-Blick, N., and Pekar, S. F., 2005, The phanerozoic record of global sea-level change: Science, v. 310, no. 5752, p. 1293-1298.

Nittrouer, J. A., 2013, Backwater hydrodynamics and sediment transport in the lowermost Mississippi River Delta: Implications for the development of fluvial-deltaic landforms in a large lowland river: IAHS-AISH Publ, v. 358, p. 48-61.

Posamentier, H. W., Allen, G. P., James, D. P., and Tesson, M., 1992, Forced regressions in a sequence stratigraphic framework: concepts, examples, and exploration significance: AAPG bulletin, v. 76, no. 11, p. 1687-1709.

Posamentier, H. W., and Vail, P. R., 1988, Eustatic controls on clastic deposition II - sequence and systems tract models, *in* Wilgus, C. K., Hastings, B. S., Posamentier, H. P., Van Wagoner, J. V., Ross, C. A., and Kendall, C. G. S. C., eds., Sea-Level Changes, SEPM special publicaiton 42, p. 125-154.

Straub, K. M., Paola, C., Mohrig, D., Wolinsky, M. A., and George, T., 2009, Compensational stacking of channelized sedimentary deposits: Journal of Sedimentary Research, v. 79, no. 9, p. 673-688.

Trampush, S., Hajek, E., Straub, K., and Chamberlin, E., 2017, Identifying autogenic sedimentation in fluvial-deltaic stratigraphy: Evaluating the effect of outcrop-quality data on the compensation statistic: Journal of Geophysical Research-Earth Surface, v. 122, p. 1-23.

Yu, L., Li, Q., and Straub, K. M., 2017, Scaling the Response of Deltas To Relative-Sea-Level Cycles By Autogenic Space and Time Scales: A Laboratory Study: Journal of Sedimentary Research, v. 87, no. 8, p. 817-837.

Alley, R.B., **Clark, P.U.**, **Huybrechts, P.** and **Joughin, I.** (2005) Ice-sheet and sea-level changes. *science*, **310**, 456–460.

Anderson, J.B., **Wallace, D.J.**, **Simms, A.R.**, **Rodriguez, A.B.**, **Weight, R.W.** and **Taha, Z.P.** (2016) Recycling sediments between source and sink during a eustatic cycle: Systems of late Quaternary northwestern Gulf of Mexico Basin. *Earth-science reviews*, **153**, 111–138.

Best, J.L. and **Ashworth, P.J.** (1997) Scour in large braided rivers and the recognition of sequence stratigraphic boundaries. *Nature*, **387**, 275–277.

Bhattacharya, J.P. (2011) Practical problems in the application of the sequence stratigraphic method and key surfaces: integrating observations from ancient fluvial-deltaic wedges with Quaternary and modelling studies. *Sedimentology Sedimentology*, **58**, 120–169.

Blum, M., **Martin, J.**, **Milliken, K.** and **Garvin, M.** (2013) Paleovalley systems: insights from Quaternary analogs and experiments. *Earth-Science Reviews*, **116**, 128–169.

Blum, M.D. and **Törnqvist, T.E.** (2000) Fluvial responses to climate and sea-level change: a review and look forward. *Sedimentology Sedimentology*, **47**, 2–48.

Burgess, P.M., **Masiero, I.**, **Toby, S.C.** and **Duller, R.A.** (2019) A Big Fan of Signals? Exploring Autogenic and Allogenic Process and Product In a Numerical Stratigraphic Forward Model of Submarine-Fan Development. *Journal of Sedimentary Research*, **89**, 1–12.

Castelltort, S. and **Van den Driessche, J.** (2003) How plausible are high-frequency sediment supply-driven cycles in the stratigraphic record? *Sediment Geol*, **157**, 3–13.

Catuneanu, O., **Abreu, V.**, **Bhattacharya, J.P.**, **Blum, M.D.**, **Dalrymple, R.W.**, **Eriksson, P.G.**, **Fielding, C.R.**, **Fisher, W.L.**, **Galloway, W.E.**, **Gibling, M.R.**, **Giles, K.A.**, **Holbrook, J.M.**, **Jordan, R.**, **Kendall, C.G.St.C.**, **Macurda, B.**, **Martinsen, O.J.**, **Miall, A.D.**, **Neal, J.E.**, **Nummedal, D.**, **Pomar, L.**, **Posamentier, H.W.**, **Pratt, B.R.**, **Sarg, J.F.**, **Shanley, K.W.**, **Steel, R.J.**, **Strasser, A.**, **Tucker, M.E.** and **Winker, C.** (2009) Towards the standardization of sequence stratigraphy. *Earth-Science Reviews*, **92**, 1–33.

Clark, P.U., **McCabe, A.M.**, **Mix, A.C.** and **Weaver, A.J.** (2004) Rapid rise of sea level 19,000 years ago and its global implications. *Science*, **304**, 1141–1144.

Fairbanks, R.G. (1989) A 17,000-year glacio-eustatic sea level record: influence of glacial melting rates on the Younger Dryas event and deep-ocean circulation. *Nature*, **342**, 637–642.

Fernandes, A.M., **Törnqvist, T.E.**, **Straub, K.M.** and **Mohrig, D.** (2016) Connecting the backwater hydraulics of coastal rivers to fluvio-deltaic sedimentology and stratigraphy. *Geology*, **44**, 979–982.

Fisk, N.H. (1954) Late Quaternary deltaic deposits of the Mississippi River. In: *Geological Society of America Special*, 62, 279–302.

Ganti, V., **Lamb, M.P.** and **Chadwick, A.J.** (2019) Autogenic Erosional Surfaces in Fluvio-deltaic Stratigraphy from Floods, Avulsions, and Backwater Hydrodynamics. *Journal of Sedimentary Research*, **89**, 815–832.

Gibling, M.R. (2006) Width and thickness of fluvial channel bodies and valley fills in the geological record: a literature compilation and classification. *Journal of Sedimentary Research*, **76**, 731–770.

Haq, B.U. (1991) Sequence stratigraphy, sea-level change, and significance for the deep sea. *Sedimentation, Tectonics and Eustasy: Sea-Level Changes at Active Margins*, 1–39.

Haq, B.U., **Hardenbol, J.** and **Vail, P.R.** (1987) Chronology of fluctuating sea levels since the Triassic. *Science*, **235**, 1156–1167.

Jelgersma, S. (1961) Holocene sea-level changes in the Netherlands.

Jerolmack, D.J. and **Paola, C.** (2010) Shredding of environmental signals by sediment transport. *Geophysical Research Letters*, **37**, L19401.

Khan, N.S., **Horton, B.P.**, **Engelhart, S.**, **Rovere, A.**, **Vacchi, M.**, **Ashe, E.L.**, **Törnqvist, T.E.**, **Dutton, A.**, **Hijma, M.P.** and **Shennan, I.** (2019) Inception of a global atlas of sea levels since the Last Glacial Maximum. *Quaternary Science Reviews*, **220**, 359–371.

Lamb, M.P., **Nittrouer, J.A.**, **Mohrig, D.** and **Shaw, J.** (2012) Backwater and river plume controls on scour upstream of river mouths: Implications for fluvio-deltaic morphodynamics.

Lazarus, E.D., **Harley, M.D.**, **Blenkinsopp, C.E.** and **Turner, I.L.** (2019) Environmental signal shredding on sandy coastlines. *Earth Surface Dynamics*, **7**, 77–86.

Li, Q., **Yu, L.** and **Straub, K.M.** (2016) Storage thresholds for relative sea-level signals in the stratigraphic record. *Geology*, **44**, 179–182.

Miller, K.G., **Kominz, M.A.**, **Browning, J.V.**, **Wright, J.D.**, **Mountain, G.S.**, **Katz, M.E.**, **Sugarman, P.J.**, **Cramer, B.S.**, **Christie-Blick, N.** and **Pekar, S.F.** (2005) The phanerozoic record of global sea-level change. *Science Science*, **310**, 1293–1298.

Mohrig, D., **Heller, P.L.**, **Paola, C.** and **Lyons, W.J.** (2000) Interpreting avulsion process from ancient alluvial sequences: Guadalope-Matarranya (northern Spain) and Wasatch Formation (western Colorado). *Geoogical Society of America Bulletin*, **112**, 1787–1803.

Nittrouer, J.A. (2013) Backwater hydrodynamics and sediment transport in the lowermost Mississippi River Delta: Implications for the development of fluvial-deltaic landforms in a large lowland river. *IAHS-AISH Publ*, **358**, 48–61.

Olariu, C. and **Bhattacharya, J.P.** (2006) Terminal distributary channels and delta front architecture of river-dominated delta systems. *J Sediment Res J Sediment Res*, **76**, 212–233.

Posamentier, H. and **Allen…, G.** (1992) High Resolution Sequence Stratigraphy--The East Coulee Delta, Alberta.

Posamentier, H.W. and **Vail, P.R.** (1988) Eustatic Controls on Clastic Deposition II—sequence and Systems Tract Models. *SEPM Special Publications*, 125–154.

Romans, B.W., **Castelltort, S.**, **Covault, J.A.**, **Fildani, A.** and **Walsh, J.** (2016) Environmental signal propagation in sedimentary systems across timescales. *Earth-Science Reviews*, **153**, 7–29.

Straub, K.M., **Paola, C.**, **Mohrig, D.**, **Wolinsky, M.A.** and **George, T.** (2009) Compensational stacking of channelized sedimentary deposits. *Journal of Sedimentary Research*, **79**, 673–688.

Törnqvist, T.E., **Wortman, S.R.**, **Mateo, Z.R.P.**, **Milne, G.A.** and **Swenson, J.B.** (2006) Did the last sea level lowstand always lead to cross-shelf valley formation and source-to-sink sediment flux?

Trower, E.J., **Ganti, V.**, **Fischer, W.W.** and **Lamb, M.P.** (2018) Erosional surfaces in the Upper Cretaceous Castlegate Sandstone (Utah, USA): Sequence boundaries or autogenic scour from backwater hydrodynamics? *Geology*, **46**, 707–710.

Vail, P.R. (1987) Seismic stratigraphy interpretation utilizing sequence stratigraphy Part 1 - Seismic stratigraphy interpretation procedure. In: *Atlas of Seismic Stratigraphy: American Association of Petroleum Geologists studies in geology* (Ed. W.W. Bally), 27, 1–10.

Van Wagoner, J., **Posamentier, H.**, **Mitchum, R.**, **Vail, P.**, **Sarg, J.**, **Loutit, T.** and **Hardenbol, J.** (1988) An overview of the fundamentals of sequence stratigraphy and key definitions.

Van Wagoner, J.C. (1995) Sequence stratigraphy and marine to nonmarine facies architecture of foreland basin strata, Book Cliffs, Utah, U.S.A. In: *Sequence Stratigraphy of Foreland Basin Deposits: Outcrop and Subsurface Examples from the Createaceous of North America, Volume 64, American Association of Petroleum Geologists, Memoirs* (Ed. J.C. Van Wagoner and G.T. Bertram), 137–223.

Voller, V.R., **Ganti, V.**, **Paola, C.** and **Foufoula-Georgiou, E.** (2012) Does the flow of information in a landscape have direction? Geophysical Research Letters. doi: 10.1029/2011GL050265

Yu, L., **Li, Q.** and **Straub, K.M.** (2017) Scaling the Response of Deltas To Relative-Sea-Level Cycles By Autogenic Space and Time Scales: A Laboratory Study. *Journal of Sedimentary Research*, **87**, 817–837.